

# Quadrupole Moments of Wobbling Excitations in $^{163}\text{Lu}$

A. Gorgen,<sup>1,2</sup> R.M. Clark,<sup>1</sup> M. Cromaz,<sup>1</sup> P. Fallon,<sup>1</sup> G.B. Hagemann,<sup>3</sup> H. Hubel,<sup>4</sup> I.Y. Lee,<sup>1</sup> A.O. Macchiavelli,<sup>1</sup>  
G. Sletten,<sup>3</sup> D. Ward,<sup>1</sup> and R. Bengtsson<sup>5</sup>

<sup>1</sup>*Nuclear Science Division, Lawrence Berkeley National Laboratory, Berkeley, California 94720*

<sup>2</sup>*DAPNIA/SPhN, CEA Saclay, F-91191 Gif-sur-Yvette, France*

<sup>3</sup>*The Niels Bohr Institute, Blegdamsvej 17, DK-2100 Copenhagen Ø, Denmark*

<sup>4</sup>*HISKP, Universitat Bonn, Nussallee 14-16, D-53115 Bonn, Germany*

<sup>5</sup>*Department of Mathematical Physics, Lund Institute of Technology, S-22362 Lund, Sweden*

(August 7, 2003)

Lifetimes of states in the triaxial strongly deformed bands of  $^{163}\text{Lu}$  have been measured in a Gammasphere experiment using the Doppler-shift attenuation method. The bands are interpreted as wobbling-phonon excitations from the characteristic electromagnetic properties of the transitions connecting the bands. Quadrupole moments were extracted for the 0-phonon yrast band and, for the first time, for the 1-phonon wobbling band. The very similar results found for both bands suggest a similar intrinsic structure confirming the wobbling interpretation. While the in-band quadrupole moments for the bands show a decreasing trend towards higher spin, the strength of the inter-band transitions remains constant. Both features can be understood by a small increase in triaxiality towards higher spin. Such a change in triaxiality is also found in cranking calculations, to which the experimental results are compared.

PACS numbers: 21.10.Tg; 21.60.Ev; 23.20.Lv; 27.70.+q

Stable triaxiality in nuclei and related phenomena have long been predicted but are difficult to prove experimentally. A region of stable triaxiality is predicted in the neutron-deficient Lu and Hf isotopes around  $N = 94$ , where cranking calculations give triaxial minima at large deformation (triaxial strongly deformed, TSD) with  $(\epsilon_2, \gamma) \approx (0.4, \pm 20^\circ)$  in the total energy surfaces. These nuclides have been studied extensively and many rotational structures that can be associated with TSD minima have been observed in several nuclides. The first proof of stable triaxiality was not the observation of these bands as such, but rather from that fact that some of the bands in odd-mass Lu isotopes can be described as wobbling-phonon excitations [1–4].

The wobbling motion is an excitation mode unique to a triaxial body. While the nucleus favors the rotation about the axis with the largest moment of inertia, it can transfer a quantized amount of angular momentum to the other axes, resulting in a sequence of rotational bands built on the same intrinsic structure. In the high-spin limit the energies of the wobbling bands can be separated into rotation about the principal axis and the wobbling motion [5]:  $E_R(I, n_w) = I(I+1)/(2\mathfrak{I}_x) + \hbar\omega_w(n_w + 1/2)$ , where  $n_w$  is the wobbling phonon number and  $\omega_w$  the wobbling frequency which depends only on the three moments of inertia. A characteristic fingerprint of the wobbling mode is the occurrence of E2 inter-band transitions with  $\Delta I = \pm 1\hbar$  from bands with  $n_w$  wobbling phonons to bands with  $n_w - 1$ . The strength of the collective inter-band transitions  $B(E2; n_w \rightarrow n_w - 1)$  is expected to be proportional to  $n_w/I$ . The presence of a particle with its spin aligned to the rotation axis, an  $i_{13/2}$  proton in the case of the TSD bands in odd-mass Lu isotopes, adds an additional degree of freedom to the wobbling motion, and

its presence may stabilize the triaxial core. The influence of the aligned proton has been studied in particle-rotor calculations [6,7].

The wobbling mode was first reported in  $^{163}\text{Lu}$  [1,2], where three TSD bands were identified as the 0-, 1-, and 2-phonon bands, with the evidence based on the characteristic properties of the inter-band transitions, for which the E2 strength of the  $\Delta I = 1$  transitions was shown to exhibit the expected pattern. Shortly afterwards, similar evidence for the wobbling mode was found in  $^{165}\text{Lu}$  [3],  $^{167}\text{Lu}$  [4], and possibly also in  $^{161}\text{Lu}$  [8].

It is interesting to note that cranking calculations predict the Hf isotopes around  $^{166}\text{Hf}$  to be even better candidates for TSD bands [9]. Experimental evidence for such bands, however, exists only in  $^{168}\text{Hf}$  [10],  $^{170}\text{Hf}$  [11], and, surprisingly, in  $^{174}\text{Hf}$  [12]. There is a discrepancy between the theoretical prediction of the region of TSD bands and where they are experimentally found. More experimental information is needed to determine the exact position of the intruder subshells which lead to the occurrence of triaxial minima.

Lifetime measurements in the excited TSD bands provide a crucial test for the wobbling interpretation. Very similar B(E2) strengths for the in-band transitions are expected, as the wobbling bands are built on the same intrinsic structure. Measurements have been attempted in  $^{163}\text{Lu}$  [13–15], but only for the yrast band and the different experiments are not in agreement.

In this letter we present data on a precision lifetime measurement in  $^{163}\text{Lu}$ , which provides the first measurement for the proposed 1-phonon wobbling band (TSD2) and resolves the discrepancy in previous data on TSD1. These new data will be used to gain important insight into the evolution of triaxiality as a function of spin that

can simultaneously explain the observed spin dependence of the in-band and inter-band  $B(E2)$  values.

High-spin states in  $^{163}\text{Lu}$  were populated in the reaction  $^{123}\text{Sb}(^{44}\text{Ca},4n)$  at a beam energy of 190 MeV. The beam was accelerated by the 88-Inch Cyclotron of the Lawrence Berkeley National Laboratory. The target comprised a  $1\text{ mg/cm}^2$  foil of  $^{123}\text{Sb}$  enriched to 99.3% on a gold backing of  $12\text{ mg/cm}^2$  to slow down and finally stop the recoils. Gamma rays were detected with the Gammasphere array [16] which for this experiment consisted of 102 large-volume Compton-suppressed germanium detectors grouped into 17 rings that cover angles from  $17.3^\circ$  to  $162.7^\circ$  with respect to the beam direction. A total of  $1.6 \times 10^9$  events in which at least five germanium detectors gave coincident signals were recorded in three days and stored in an indexed, energy-ordered database using the BLUE software [17]. Angle-dependent spectra were sorted from the database under various gating conditions.

The level lifetimes were extracted by the analysis of the Doppler-broadened lineshapes observed at various angles with respect to the beam direction. The codes of Wells and Johnson [18], based on the code of Bacelar [19], was used for this analysis. The stopping of the recoils was simulated using Monte Carlo methods with 5000 histories and a time step of 0.001 ps following the prescription of Gascon et al. [20]. For the electronic stopping power the tables of Northcliffe and Shilling [21] were used with a shell correction. Lineshapes were fitted simultaneously for multiple transitions and different combinations of angles. The side feeding was modeled by a cascade of five transitions with the same moment of inertia as the in-band transitions. The intensity of the side feeding was constrained to the experimentally observed value. It was difficult to determine the side-feeding intensity for the states in the upper part of the bands where the lineshapes are very broad. In these cases the intensities were taken from an earlier thin-target experiment [22]. This is justified since the intensities for the transitions lower in the bands agree well. The quadrupole moment for transitions feeding into the bands was allowed to vary only within 15% of that of the in-band transitions for initial fits of single states and it was fixed to that value for the subsequent fits of the entire cascade. Such a constraint has been found to be a reasonable assumption in earlier lifetime measurements of TSD bands [14]. Furthermore, for some transitions in band TSD1 it was possible to gate from above, eliminating the effects of side feeding. The results obtained when gating from above and gating from below with the above side-feeding model were in good agreement. The influence of the direct feeding from TSD2 into TSD1 was neglected since this accounts only for about 5% of the total feeding and the lifetimes in band TSD2 are very similar to those in TSD1, as will be shown. Other fit parameters include a linear background and the intensities of contaminant peaks. These

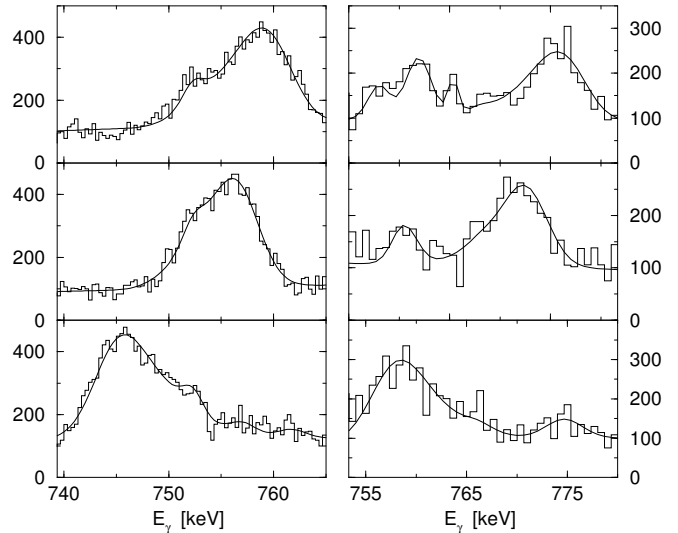


FIG. 1. Spectra and fitted lineshapes for the 753 keV transition of band TSD1 (left) and for the 766 keV transition of band TSD2 (right) observed at  $50^\circ$  (top),  $70^\circ$  (center), and  $130^\circ$  (bottom). Contaminant peaks are present and included in the fit.

parameters were also determined in an initial fit to the individual transitions and then fixed for subsequent fits to multiple transitions. The errors were derived from the covariance matrix of the  $\chi^2$  minimization and from the spread of the results obtained for different combinations of angles. Systematic errors originating from the choice of stopping powers are not included. Examples of typical lineshape fits for transitions in bands TSD1 and TSD2 are shown in Fig. 1.

Eight lifetimes of states in TSD1 and seven in TSD2 were determined from the Doppler-broadened line shapes. The results are summarized in Tab. I. The values for TSD1 agree within errors with the earlier measurement of Schönwaßer et al. [14], in which the transition quadrupole moments of the 752, 805, and 858 keV transitions were found to be  $8.1_{-1.1}^{+1.0}$ ,  $8.3_{-1.1}^{+1.9}$ , and  $8.0_{-1.5}^{+1.6}$  eb, respectively. They are, however, in disagreement with the much larger values reported by Schmitz et al. [13]. It has been speculated [14] that this discrepancy is due to an inconsistent treatment of the side feeding in ref. [13]. Due to the far higher efficiency of the Gammasphere spectrometer compared to GaSp and Nordball, with which the earlier data were taken, the new data have smaller uncertainties. In the present data there are about 15 times more counts in the peaks (for each angle) compared to the GaSp data [14], and about 35 times more than in the Nordball data [13]. In addition, data at more angles were recorded in the present experiment. We now feel that the weight of evidence is against the results reported by Schmitz et al. [13].

While the measured lifetimes in band TSD1 can be directly converted into the  $B(E2)$  strength, the ones measured in TSD2 have to be corrected for the competing

TABLE I. Lifetimes,  $B(E2)$  values, and transition quadrupole moments  $Q_t$  for the in-band transitions in bands TSD1 and TSD2.

$I_i^{\pi}$	$E_{\gamma}$ [keV]	$\tau$ [ps]	$B(E2)$ [ $e^2b^2$ ]	$Q_t$ [ $e^2b^2$ ]
41/2 <sup>+</sup>	578.6	0.364 <sup>+0.073</sup> <sub>-0.085</sub>	3.45 <sup>+0.80</sup> <sub>-0.69</sub>	9.93 <sup>+1.14</sup> <sub>-0.99</sub>
45/2 <sup>+</sup>	639.0	0.250 <sup>+0.035</sup> <sub>-0.039</sub>	3.07 <sup>+0.48</sup> <sub>-0.43</sub>	9.34 <sup>+0.72</sup> <sub>-0.65</sub>
49/2 <sup>+</sup>	697.0	0.202 <sup>+0.021</sup> <sub>-0.023</sub>	2.45 <sup>+0.28</sup> <sub>-0.25</sub>	8.32 <sup>+0.47</sup> <sub>-0.42</sub>
53/2 <sup>+</sup>	752.6	0.119 <sup>+0.009</sup> <sub>-0.010</sub>	2.84 <sup>+0.24</sup> <sub>-0.22</sub>	8.93 <sup>+0.38</sup> <sub>-0.35</sub>
57/2 <sup>+</sup>	805.6	0.096 <sup>+0.011</sup> <sub>-0.012</sub>	2.50 <sup>+0.32</sup> <sub>-0.29</sub>	8.37 <sup>+0.54</sup> <sub>-0.49</sub>
61/2 <sup>+</sup>	857.7	0.088 <sup>+0.010</sup> <sub>-0.011</sub>	1.99 <sup>+0.26</sup> <sub>-0.23</sub>	7.45 <sup>+0.43</sup> <sub>-0.43</sub>
65/2 <sup>+</sup>	909.7	0.067 <sup>+0.010</sup> <sub>-0.015</sub>	1.95 <sup>+0.44</sup> <sub>-0.30</sub>	7.37 <sup>+0.82</sup> <sub>-0.57</sub>
69/2 <sup>+</sup>	962.5	0.047 <sup>+0.017</sup> <sub>-0.011</sub>	2.10 <sup>+0.80</sup> <sub>-0.48</sub>	7.63 <sup>+1.46</sup> <sub>-0.88</sub>
47/2 <sup>+</sup>	654.6	0.215 <sup>+0.037</sup> <sub>-0.048</sub>	2.56 <sup>+0.57</sup> <sub>-0.44</sub>	8.51 <sup>+0.95</sup> <sub>-0.73</sub>
51/2 <sup>+</sup>	711.2	0.144 <sup>+0.017</sup> <sub>-0.022</sub>	2.67 <sup>+0.41</sup> <sub>-0.33</sub>	8.67 <sup>+0.66</sup> <sub>-0.53</sub>
55/2 <sup>+</sup>	766.2	0.095 <sup>+0.013</sup> <sub>-0.018</sub>	2.81 <sup>+0.53</sup> <sub>-0.41</sub>	8.88 <sup>+0.83</sup> <sub>-0.64</sub>
59/2 <sup>+</sup>	819.9	0.087 <sup>+0.026</sup> <sub>-0.037</sub>	2.19 <sup>+0.94</sup> <sub>-0.65</sub>	7.82 <sup>+1.66</sup> <sub>-1.15</sub>
63/2 <sup>+</sup>	872.9	0.064 <sup>+0.013</sup> <sub>-0.021</sub>	2.23 <sup>+0.75</sup> <sub>-0.48</sub>	7.91 <sup>+1.32</sup> <sub>-0.84</sub>
67/2 <sup>+</sup>	926.5	0.075 <sup>+0.017</sup> <sub>-0.025</sub>	1.60 <sup>+0.52</sup> <sub>-0.37</sub>	6.66 <sup>+1.09</sup> <sub>-0.76</sub>
71/2 <sup>+</sup>	980.2	0.056 <sup>+0.017</sup> <sub>-0.029</sub>	1.61 <sup>+0.82</sup> <sub>-0.49</sub>	6.68 <sup>+1.70</sup> <sub>-1.02</sub>

decay out in order to get the strength of the in-band transitions. Since it is difficult to obtain the branching ratios from the Doppler-broadened peaks, the values obtained in the thin-target experiment [22] were used to correct for the decay out. For axial symmetric nuclei, quadrupole moments can be extracted from the  $B(E2)$  values using  $B(E2) = \frac{5}{16\pi} Q^2 \langle I_i K 20 | I_f K \rangle^2$ . For a triaxial nucleus  $K$  is not a good quantum number and, instead, a distribution of  $K$  values assuming that the  $i_{13/2}$  proton is fully aligned with the rotational axis has been used. The  $K$  distribution can be calculated using Wigner's  $D$ -function. The resulting in-band quadrupole moments are summarized in Tab. I and plotted in Fig. 2.

The values for the two bands show a striking similarity. This is expected in the wobbling-phonon picture, as the bands are built on the same intrinsic structure. One would expect a difference of only about 4% in the

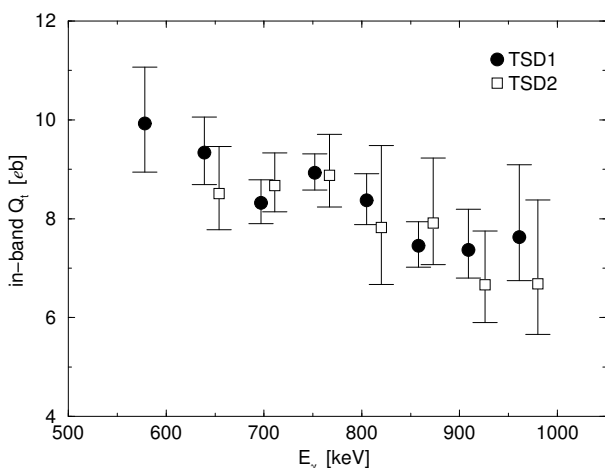


FIG. 2. Transition quadrupole moments of the in-band transitions in bands TSD1 and TSD2.

quadrupole moments due to the tilting of the core angular momentum for the 1-phonon wobbling band and therefore slightly different vector coupling coefficients. The identity of the quadrupole moments cannot stand as a proof alone, but is a necessary condition to be fulfilled by wobbling bands and is, therefore, further evidence for the wobbling motion and stable triaxiality.

Both bands exhibit a decrease in the  $B(E2)$  and  $Q_t$  values as the spin increases. The fact that both bands have not only very similar values, but also show the same change of these values further strengthens the argument that the bands are built on the same structure. The observed decrease in the in-band transition strengths will also be important to understand the spin dependence of the inter-band transition strengths, which is one of the key observable signatures of the wobbling motion.

In order to understand the decrease of the  $Q_t$ , cranking calculations have been performed with the *Ultimate Cranker* code [23]. The quadrupole moments calculated from the wave functions are compared to the experimental values for TSD1 in the upper part of Fig. 3. This comparison allows to associate the band with the second minimum at  $(\epsilon_2, \gamma) \approx (0.4, +20^\circ)$ . The calculated quadrupole moment for the normal deformed minimum at  $(\epsilon_2, \gamma) \approx (0.2, 0^\circ)$  is shown for comparison. The calculations reproduce a small decrease in the quadrupole moment due to an increase in the triaxiality parameter  $\gamma$  from  $\sim 19.5^\circ$  to  $\sim 21.5^\circ$  and a slight decrease in quadrupole deformation  $\epsilon_2$  from  $\sim 0.40$  to  $\sim 0.38$ . This is illustrated in the lower part of Fig. 3. However, the decrease in the calculations is not as pronounced as in the experimental data.

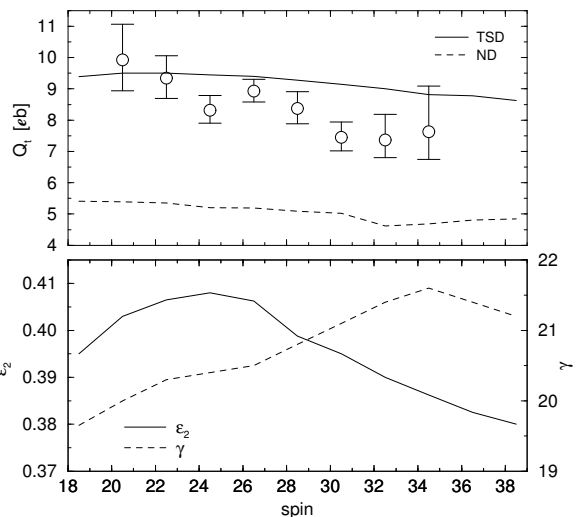


FIG. 3. Comparison of the transition quadrupole moments with cranking calculations for the TSD and the normal deformed minimum (upper panel). The lower panel shows the quadrupole deformation (solid line) and triaxiality (dashed line) at the minimum in the total energy surface as a function of spin.

TABLE II. B(E2) and B(M1) values for the connecting transitions from TSD2 to TSD1.

$I_i^\pi$	$E_\gamma$ [keV]	B(E2) [ $e^2b^2$ ]	B(M1) [ $\mu_N^2$ ]
47/2 <sup>+</sup>	658.9	0.54 <sup>+0.13</sup> <sub>-0.11</sub>	0.017 <sup>+0.006</sup> <sub>-0.005</sub>
51/2 <sup>+</sup>	673.2	0.54 <sup>+0.09</sup> <sub>-0.08</sub>	0.017 <sup>+0.005</sup> <sub>-0.005</sub>
55/2 <sup>+</sup>	686.8	0.70 <sup>+0.18</sup> <sub>-0.15</sub>	0.024 <sup>+0.008</sup> <sub>-0.007</sub>
59/2 <sup>+</sup>	701.1	0.65 <sup>+0.34</sup> <sub>-0.26</sub>	0.023 <sup>+0.013</sup> <sub>-0.011</sub>
63/2 <sup>+</sup>	716.3	0.66 <sup>+0.29</sup> <sub>-0.24</sub>	0.024 <sup>+0.012</sup> <sub>-0.010</sub>

The new lifetime results for band TSD2 allow, for the first time, to establish the absolute B(E2) and B(M1) values for the transitions connecting bands TSD2 and TSD1. They are shown in Tab. II, where an average value of the mixing ratio  $\delta = -3.10_{-0.36}^{+0.44}$  was used, taken from measurements of the angular correlation and linear polarization of the transitions [1,22]. This average value did not vary significantly up to spin 51/2 and was used to extract the B(E2) and B(M1) values at higher spins.

Due to the combined uncertainties of the lifetimes, the branching ratios [22], and the mixing ratio [1], the errors are too large to determine the spin dependence of the inter-band B(E2) strengths, which in the wobbling picture should be proportional to  $n_w/I$ . However, it is possible to use the ratio of the inter-band to in-band B(E2) values for which the uncertainties of the lifetimes do not enter, and compare them to the particle-rotor calculations [6,7]. This is illustrated in Fig. 4. The B(E2) ratios are constant and do not follow the expected dependence on spin. However, this ratio strongly depends on the triaxiality parameter  $\gamma$ , as  $B(E2;out) \propto \sin^2(\gamma + 30^\circ)$  and  $B(E2;in) \propto \cos^2(\gamma + 30^\circ)$ . Together with the results for the in-band transitions this behavior indicates a stronger increase in triaxiality towards higher spin than found in the calculations. An increase from  $\gamma \approx 16^\circ$  to  $\gamma \approx 22^\circ$  would explain the pronounced decrease in the in-band quadrupole moments and, at the same time, the constant B(E2) ratio for the out-band transitions, so that a consistent overall description of the new experimental data is reached.

In summary, lifetimes of states in the TSD bands 1 and 2 in  $^{163}\text{Lu}$  were measured using the Doppler-shift attenuation method. The in-band B(E2) values and quadrupole moments for the two bands are very similar and suggest that the bands are built on the same intrinsic structure. Furthermore, the values show a decrease towards higher spin for both bands which is qualitatively reproduced by cranking calculations. The ratio of inter-band to in-band B(E2) values is found to be constant as a function of spin. We propose that the decrease in the in-band B(E2) and the constant inter-band B(E2) have the same physical origin and correspond to a stronger increase in the triaxiality than predicted by the calculations. The new results support the interpretation of the TSD bands as wobbling-phonon excitations and give an experimental

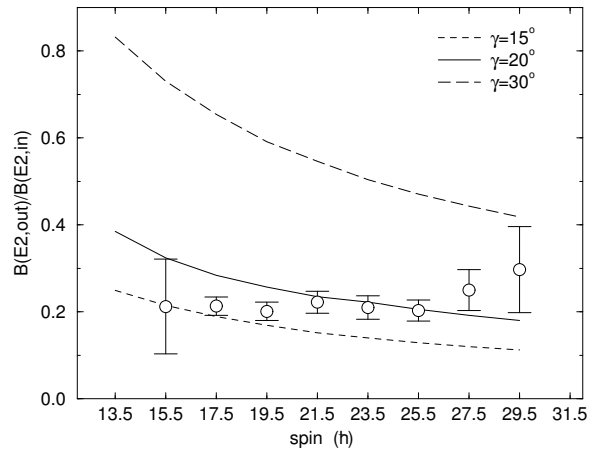


FIG. 4. Ratio of the out-band to in-band B(E2) values in comparison with particle-rotor calculations for different values of  $\gamma$ .

handle on the triaxiality parameter  $\gamma$ .

This research was supported in part by the US DoE under contract No. DE-AC03-76SF00098, the Danish Science Foundation, and the German BMBF. We wish to thank the staff of the 88-Inch Cyclotron at Berkeley, and Ikuko Hamamoto for communicating and discussing theoretical results.

- 
- [1] S.W. Ødegård et al., Phys. Rev. Lett. 86, 5866 (2001)
  - [2] D.R. Jensen et al., Phys. Rev. Lett. 89, 142503 (2002)
  - [3] G. Schönwaßer et al., Phys. Lett. B552, 9 (2003)
  - [4] H. Amro et al., Phys. Lett. B553, 197 (2003)
  - [5] A. Bohr and B. Mottelson, *Nuclear Structure*, (Benjamin, New York, 1975), Vol. II, pp. 190 ff.
  - [6] I. Hamamoto, Phys. Rev. C 65, 044305 (2002)
  - [7] I. Hamamoto, G.B. Hagemann, Phys. Rev. C 67, 014319 (2003)
  - [8] P. Bringel et al., to be published
  - [9] R. Bengtsson and H. Ryde, to be published
  - [10] H. Amro et al., Phys. Lett. B506, 39 (2001)
  - [11] A. Neußer et al., Eur. Phys. J. A 15, 439 (2002)
  - [12] M.K. Djongolov et al., Phys. Lett. B560, 24 (2003)
  - [13] W. Schmitz et al., Phys. Lett. B303, 230 (1993)
  - [14] G. Schönwaßer et al., Eur. Phys. J. A 13, 291 (2002)
  - [15] G. Schönwaßer et al., Eur. Phys. J. A 15, 435 (2002)
  - [16] I.Y. Lee, Nucl. Phys. A520, 641c (1990)
  - [17] M. Cromaz et al., Nucl. Instrum. Methods Phys. Res. A 462, 519 (2001)
  - [18] J.C. Wells and N. Johnson, private communication
  - [19] J.C. Bacelar et al., Phys. Rev. C 35, 1170 (1987)
  - [20] J. Gascon et al., Nucl. Phys. A 513, 344 (1990)
  - [21] L.C. Northcliffe and R.F. Schilling, Nucl. Data Tables 7, 233 (1970)
  - [22] D.R. Jensen et al., Nucl. Phys. A703, 3 (2002)
  - [23] T. Bengtsson, Nucl. Phys. A 512, 124 (1990)